Momentum-Resolved Observation of Thermal and Quantum Depletion in a Bose Gas

R. Chang,[1] Q. Bouton,[1] H. Cayla,[1] C. Qu,[2] A. Aspect,[1] C. I. Westbrook,[1] and D. Clément[1,*]
[1]Laboratoire Charles Fabry, Institut d'Optique, CNRS, Univ. Paris Sud,
2 Avenue Augustin Fresnel 91127 PALAISEAU cedex, France
[2]INO-CNR BEC Center and Dipartimento di Fisica, Universita di Trento, 38123 Povo, Italy
(Received 16 August 2016; published 2 December 2016)

We report on the single-atom-resolved measurement of the distribution of momenta $\hbar k$ in a weakly interacting Bose gas after a 330 ms time of flight. We investigate it for various temperatures and clearly separate two contributions to the depletion of the condensate by their k dependence. The first one is the thermal depletion. The second contribution falls off as k^{-4}, and its magnitude increases with the in-trap condensate density as predicted by the Bogoliubov theory at zero temperature. These observations suggest associating it with the quantum depletion. How this contribution can survive the expansion of the released interacting condensate is an intriguing open question.

DOI: 10.1103/PhysRevLett.117.235303

In quantum systems, intriguing many-body phenomena emerge from the interplay between quantum fluctuations and interactions. Quantum depletion is an emblematic example of such an effect, occurring in one of the simplest many-body systems: a gas of interacting bosons at zero temperature. In the absence of interactions, the ground state corresponds to all particles occupying the same single-particle state. Taking into account interparticle repulsive interactions at the mean-field level leads to a similar solution where all particles are condensed in the same one-particle state whose shape is determined by the trapping potential and interactions. In a beyond mean-field approach, which can be interpreted as taking into account quantum fluctuations and two-body interactions, the description is dramatically different. The many-body ground state consists of several components: a macroscopically occupied single-particle state, the condensate, and a population of single-particle states different from the condensate, the depletion.

This many-body description applies to diverse bosonic systems such as superfluid helium [1], exciton polaritons [2], and degenerate Bose gases [3]; it has also found analogies in phenomena such as Hawking radiation from a black hole [4] and spontaneous parametric down-conversion in optics [5]. The fraction of atoms not in the condensate at zero temperature, the quantum depletion, increases with the strength of interparticle interactions and with the density, rising up to 90% in liquid ^{4}He [1]. In ultracold gases, where the density is significantly smaller, the quantum depletion usually represents a small fraction (less than 1%) of the total population. At nonzero temperature there is an additional contribution to the population of single-particle states above the condensate, originating from the presence of thermal fluctuations.

For weakly interacting systems, Bogoliubov theory describes quantum and thermal contributions to the condensate depletion [6,7]. This approach shows that the elementary, low-energy excitations are collective quasiparticle (phonon) modes, as has been verified in experimental studies with liquid ^{4}He [8], degenerate quantum gases [9], and exciton polaritons [2]. At zero temperature, the many-body ground state is defined as a vacuum of these quasiparticle modes. When projected onto a basis of single-particle states with momentum $\hbar k$, this many-body ground state exhibits a distribution $n(k)$, which scales as k^{-4} at large k. These power law tails do not exist in mean-field descriptions, for which the momentum distribution has a finite extent. At nonzero temperature, the contribution to $n(k)$ induced by thermal fluctuations decays exponentially for energies larger than the temperature. Previous experiments with atomic gases [10,11] have observed the total depletion of the condensate after a time-of-flight expansion, but could not distinguish between the thermal and quantum contributions.

In this Letter, we report on the observation of momentum-space signatures of thermal and quantum depletion in a gas of interacting bosons. We investigate, for various temperatures and atomic densities, the three-dimensional atomic distribution after a long time of flight (see Fig. 1), i.e., the asymptotic momentum distribution. Three components can be identified (see Fig. 2): the condensate (**I**), the thermal depletion (**II**), and a tail decaying as k^{-4} and increasing with the in-trap condensate density (**III**). This suggests associating region **III** with the quantum depletion, but with two caveats. First, k^{-4} tails originated from contact interaction were observed to vanish during the expansion of interacting fermions [12]. Recent theoretical work investigating interacting bosons predicts that the k^{-4} tails adiabatically decrease with the condensate density during the expansion [13]. Second, the magnitude of the k^{-4} tails we measure is larger than the in-trap prediction of the Bogoliubov theory, by a factor of about 6. Our identification of the k^{-4} tail with the quantum depletion thus demands that there exists either a nonadiabatic process in the expansion, decoupling the in-trap k^{-4} component

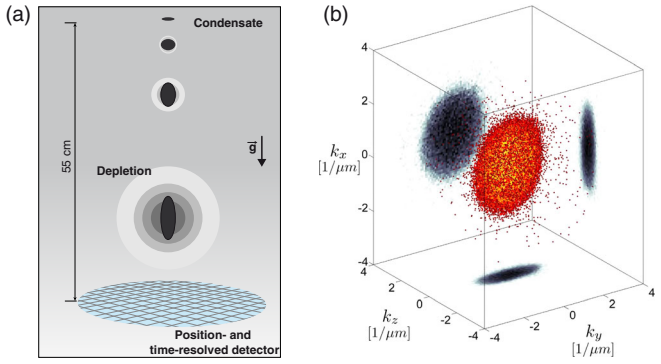

FIG. 1. (a) Sketch of cloud expansion and detection by a microchannel plate detector, yielding the 3D asymptotic momentum distribution (far-field regime). The initially cigar-shaped Helium condensate (black) undergoes anisotropic expansion, inverting its aspect ratio. Quantum depletion and/or thermally excited atoms (grays) populate momentum states beyond those associated with the condensate, and are expected to have a spherical symmetry. (b) Measured 3D distribution of atoms $n_\infty(\mathbf{k})$ after a 330 ms time of flight. The central dense part corresponds to the condensate while the isolated dots are excited particles outside of the condensate wave function. Also shown are the 2D projections, highlighting the condensate anisotropy.

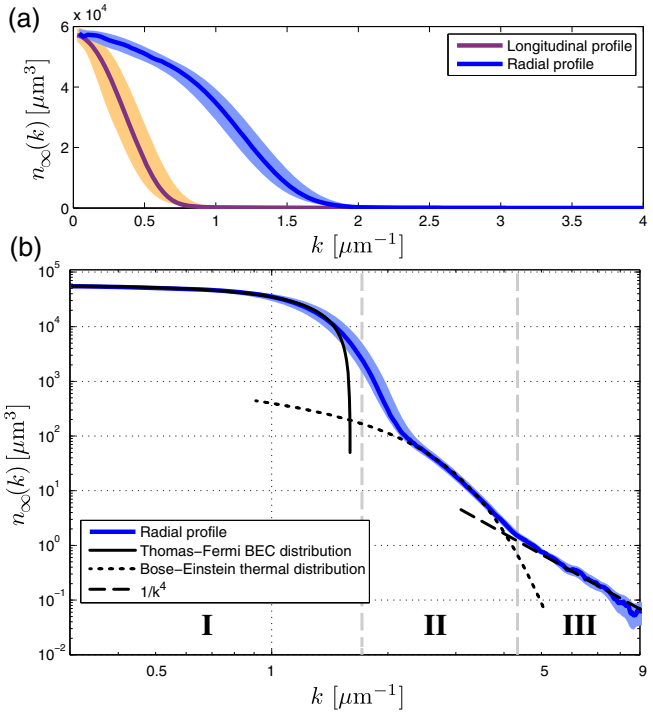

FIG. 2. 1D momentum profiles obtained from cuts of the 3D data $n_\infty(\mathbf{k})$. (a) Profiles along the radial (blue) and longitudinal (purple) directions. In linear scale, the tails are not visible. (b) Log-log scale plot of the radial profile. The solid line is the scaling solution for the condensate in the Thomas-Fermi approximation (region **I**: $k < 1.7\ \mu m^{-1}$); the dotted line is a Bose distribution fitting the thermal wings (region **II**: $1.7 < k < 4.3\ \mu m^{-1}$); the dashed line is a k^{-4} power law fitting the high-momentum tails (region **III**: $k > 4.3\ \mu m^{-1}$). Solid lines are a smoothed average of the density data, and the lightly shaded band is the running standard deviation. The dark count rate corresponds to a level less than $\sim 10^{-2}\ \mu m^3$, which is 1 order of magnitude below the lowest data point. The plotted range of momenta is limited by the physical size of the detector.

from the expanding condensate, or an interaction-induced effect beyond the mean-field description of the expansion, leading to $1/k^4$ tails.

Our experiment is performed with a Bose-Einstein condensate of metastable helium-4 atoms (^{4}He*). Cigar-shaped condensates, of typically $N = 2 \times 10^5$ ^{4}He* atoms in the polarized 2^3S_1, $m_J = +1$ state are produced in an optical dipole trap with trapping frequencies $\omega/2\pi = (438, 419, 89)$ Hz [14,15]. After abruptly turning off the optical trap (in less than 2 μs) we detect the gas with a microchannel plate (MCP) [16,17], after a 55 cm free fall corresponding to a time of flight (TOF) of ~330 ms. A radio-frequency (rf) ramp transfers a fraction of the polarized $m_J = +1$ atoms to the nonmagnetic $m_J = 0$ state after 2 ms of TOF (see Ref. [18] for details). The presence of a magnetic gradient after the RF ramp ensures that only $m_J = 0$ atoms fall onto the MCP and can be detected. The MCP allows us to detect ^{4}He* atoms individually and to record the two-dimensional (2D) position and the arrival time of each atom in the plane of the detector. The arrival time of each atom directly translates into a vertical coordinate, so that we reconstruct the complete 3D atoms distribution, in contrast with the usual optical imaging that yields a 2D column-integrated density. Another advantage of a MCP operated in the counting mode is its extremely low dark count rate. Here it allows us to investigate the atomic density over more than 5 decades (see below).

The detector is placed 55 cm below the trapped cloud [see Fig. 1(a)], so that after switching off the trap, the observation is made in the far-field regime where finite-size effects of the source can be safely neglected. In the free-falling frame of reference, we thus identify the position $\mathbf{r}$ of a detected atom (with respect to the cloud center) with a momentum component $\mathbf{k} = m\mathbf{r}/\hbar\bar{t}$, where $\bar{t} = 330$ ms is the time of flight of the cloud center [18]. This yields the asymptotic momentum distribution $n_\infty(\mathbf{k})$ obtained from the density distribution of the expanding cloud $n(\mathbf{r}, \bar{t})$, according to the ballistic relationship

$$n_\infty(\mathbf{k}) = (\hbar\bar{t}/m)^3 n(\mathbf{r}, \bar{t}). \quad (1)$$

The distribution $n_\infty(\mathbf{k})$ should not be confused with the in-trap momentum distribution $n(\mathbf{k})$, since the initial stage of the expansion is affected by interatomic interactions. Nevertheless, as we argue below, the high-momentum tails of $n_\infty(\mathbf{k})$ provide interesting information on the in-trap momentum distribution $n(\mathbf{k})$.

An example of $n_\infty(\mathbf{k})$ is shown in Fig. 1(b). The main component is the pancake-shaped distribution expected

for the cigar-shaped condensate according to the mean-field description of the expansion [19,20]. We also distinguish momentum components beyond those of the condensate, with a much lower density and an isotropic distribution [18]. From 3D distributions $n_\infty(\mathbf{k})$, we obtain radial and longitudinal profiles as shown in Fig. 2 [18]. The resulting profiles exhibit three distinct regions, as illustrated in Fig. 2(b).

First, the observed distributions are dominated by the high-density condensate (region **I**: $k \equiv |\mathbf{k}| < 1.7\ \mu\mathrm{m}^{-1}$). The initial expansion of the condensate is driven by interparticle interactions, resulting in an asymptotic distribution different from the in-trap momentum distribution. This dynamics is fully captured by a mean-field treatment, the scaling solution [19,20] calculated in the Thomas Fermi approximation, as shown in Fig. 2(b). We have checked that a numerical solution of the time-dependent Gross-Pitaevskii equation for the pure condensate, beyond the Thomas Fermi approximation, yields negligible corrections [18].

Beyond the anisotropic mean-field distribution we observe high-momentum tails ($k > 1.7\ \mu\mathrm{m}^{-1}$) with spherical symmetry [18]: we attribute these components [regions **II** and **III** in Fig. 2(b)] to the depletion of the condensate. The *isotropic* character of the atomic distribution in the tails indicates that the *anisotropic* mean-field potential describing the interactions in the condensate does not play a significant role in the expansion of particles belonging to regions **II** and **III**. Thus, we assume in the following that the high-momentum components of the tails, corresponding to a kinetic energy larger than the chemical potential of the condensate, quickly escape the condensate and are not affected by the mean-field potential during the expansion. The tails are visible over three decades in density, allowing us to perform a detailed study of their momentum dependence. We observe two distinct regions: a middle region without a well-defined power-law variation (region **II**), and a high-momentum region with density varying as $k^{-\alpha}$ (region **III**). A power-law fit to the data in region **III** yields $\alpha = 4.2(2)$.

A quantitative description of the condensate depletion close to zero temperature is provided by Bogoliubov's microscopic theory, which yields a beyond mean-field model, taking into account quantum and thermal fluctuations [6,7]. In the many-body Hamiltonian, this approximated approach retains only quadratic terms in the particle operators a_k, where a_k is the operator annihilating a particle with momentum $\hbar k$. The simplified Hamiltonian can then be diagonalized by introducing the quasiparticle operators b_k defined by the Bogoliubov transformation $b_k = u_k a_k + v_{-k} a^\dagger_{-k}$ [6,7].

At zero temperature, the many-body ground state is the vacuum of quasiparticles, defined as $\langle b^\dagger_k b_k\rangle = 0$ for any $k \neq 0$. It corresponds to a nonzero population of excited single-particle states, $\langle a^\dagger_k a_k\rangle = |v_k|^2$ for $k \neq 0$. This is the quantum depletion of the Bose condensate, which has no classical analog, and can be seen as arising from the interplay of Bose statistics and interactions. At nonzero temperature, the particle occupation number of nonzero momentum k can be expressed analytically in terms of the quasiparticle occupation number:

$$n(k) = \langle a^\dagger_k a_k\rangle = (|u_k|^2 + |v_k|^2)\langle b^\dagger_k b_k\rangle + |v_k|^2, \qquad (2)$$

with the occupation number of quasiparticles given by a Bose-Einstein distribution,

$$\langle b^\dagger_k b_k\rangle = \frac{1}{\exp(\epsilon(k)/k_B T) - 1}, \qquad (3)$$

where $\epsilon(k)$ is the Bogoliubov dispersion relation, k_B is Boltzmann's constant, and T is the temperature. The interpretation of Eq. (2) is clear: the first term, proportional to $\langle b^\dagger_k b_k\rangle$, represents the thermal depletion; the second term is associated with the quantum depletion.

The particle occupation number $|v_k|^2$ corresponding to the quantum depletion varies as k^{-1} for $k\xi \ll 1$, and as k^{-4} for $k\xi \gg 1$, where ξ is the healing length of the condensate. The small k behavior is related to the Heisenberg inequality associated with the particle and the density operators [21]. The large k behavior arises due to the two-body contact interaction and is related to Tan's contact constant, a universal quantity that connects contact interactions to the thermodynamics of a many-body system [22,23]. In contrast, the depletion associated with the thermal excitations varies differently with k due to the additional term $\langle b^\dagger_k b_k\rangle$. In particular, it decays exponentially for $k\lambda_{dB} \gg 1$, where $\lambda_{dB} = \sqrt{h^2/2\pi m k_B T}$ is the de Broglie wavelength. These differences provide a means to unambiguously distinguish the quantum depletion from the thermal depletion.

The presence of an inhomogeneous trap does not modify the prediction for the condensate depletion at momenta large compared to the inverse system size $1/R \simeq 0.08\ \mu\mathrm{m}^{-1}$, where the results of Bogoliubov theory can be averaged using the local density approximation (LDA). For a harmonically trapped gas, a LDA calculation keeps the large-momentum k^{-4} scaling of the homogeneous model [18]. On the other hand, the thermal depletion distribution in a harmonic trap approaches a polylog function at high temperature [3].

To identify the contributions in regions **II** and **III**, we have investigated the tails of the measured distribution $n_\infty(k)$ as a function of temperature. Figure 3 presents the radial distributions $k^4 \times n_\infty(k)$ for clouds subjected to a controlled heating sequence [18]. Assuming the LDA average of Eq. (2), we fit the tails in Fig. 3 ($k > 2\ \mu\mathrm{m}^{-1}$) with the function $k^4 \times n_{\mathrm{fit}}(k)$, where

$$n_{\mathrm{fit}}(k) = \frac{N_{\mathrm{th}} g_{3/2}[\exp(-k^2\lambda^2_{dB}/4\pi)]}{1.202(2\pi/\lambda_{dB})^3} + \frac{\mathcal{C}_\infty}{(2\pi)^3 k^4}, \qquad (4)$$

with T_a (via $\lambda_{dB} = h/\sqrt{2\pi m k_B T_a}$), N_{th} and $\mathcal{C}_\infty$ are fitting parameters. The first term in Eq. (4) is the polylog function describing a thermal component with an atom number N_{th}

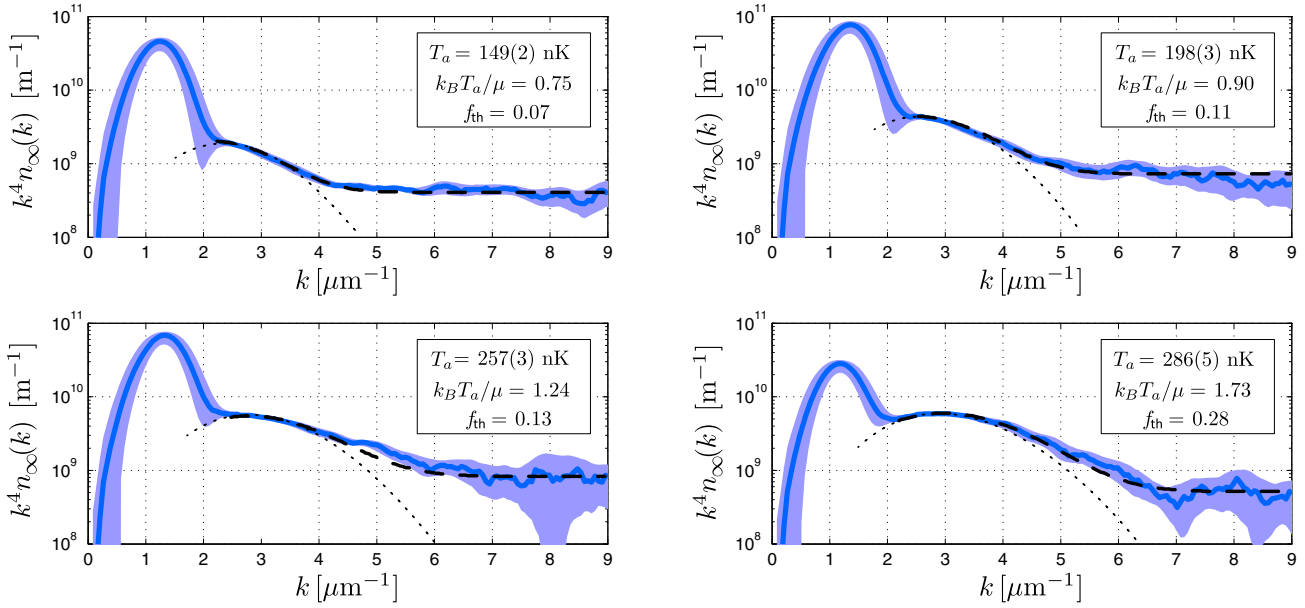

FIG. 3. Measured $k^4 n_\infty(k)$ plotted as a function of k and at various temperatures. Solid blue lines are a smoothed average of the density data, and the lightly shaded blue band shows the running standard deviation. The dashed line is a fit using Eq. (4) which involves two terms: the thermal depletion (also shown as a dotted line) and the quantum depletion revealed by the k^{-4} scaling at large k. The fitting procedure yields the temperature T_a, the thermal atom number $N_{\rm th}$ and the asymptotic constant $\mathcal{C}_\infty$. Noted in each subplot are T_a, the ratio of the thermal energy and the chemical potential $k_B T_a/\mu$ and $f_{\rm th} = N_{\rm th}/N$.

and an apparent temperature T_a [24]. The second term corresponds to a distribution decaying as $1/k^4$. The function $n_{\rm fit}(k)$ is an excellent fit to the experimental profiles (see Fig. 3). As the gas is heated, the temperature T_a and the thermal fraction $f_{\rm th} = N_{\rm th}/N$ increase. The variation of $f_{\rm th}$ with T_a/T_c (T_c being the critical temperature of condensation) is in excellent agreement with the semiclassical prediction [3], confirming our identification of region **II** with the thermal depletion. Although they represent less than ~0.5 % of the total atom number, the k^{-4} tails are clearly visible beyond the thermal component (see Fig. 3), and thus associated with a zero-temperature effect [25]. In the weakly interacting regime that we investigate, condensate lifetimes are on the order of seconds. We have measured identical k^{-4} tails when holding the atoms for an extra second in the trap, showing that the gas is at equilibrium before the release.

The presence of k^{-4} tails in a cloud released from a trap was previously reported in strongly interacting Fermi gases [12], but was not found with bosons [26]. The observation of the k^{-4} tails in a Fermi gas required ramping the interaction strength to zero before the expansion [12], on a time scale shorter than that associated with many-body effects. Recent theoretical work concluded that the k^{-4} tails should adiabatically vanish during the expansion of a Bose gas when the strength of interaction is kept constant [13]. These considerations indicate that in order to associate the observed k^{-4} tails in $n_\infty(k)$ with the quantum depletion in the trapped cloud, we must invoke a nonadiabatic process. Since the scattering length in the $m_J = 0$ state is expected to be smaller than that in the $m_J = +1$ state [18,27], a nonadiabatic transfer between these two states at the optical trap turnoff might explain our observation, but we have not yet found any evidence of this possibility in the experiment. On the other hand, there is no many-body treatment of

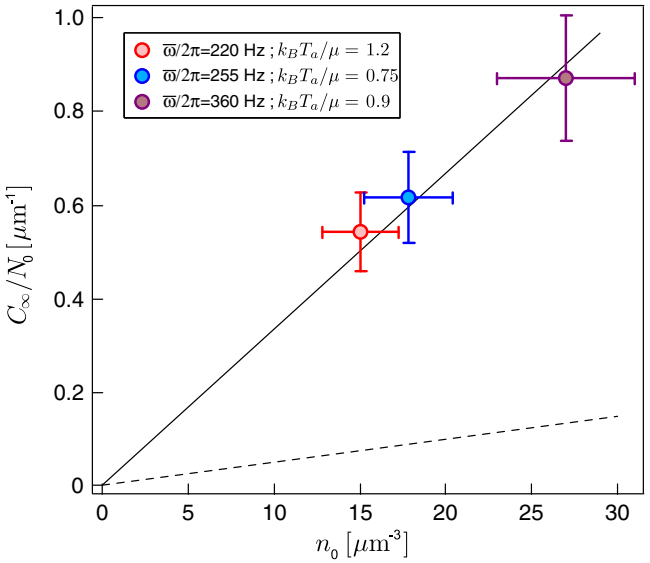

FIG. 4. Contact constant $\mathcal{C}_\infty/N_0$ per condensed particle plotted as a function of the condensate density n_0. The geometric trapping frequency $\bar{\omega}/2\pi$ and the ratio $k_B T_a/\mu$ are indicated. The dashed line is the Bogoliubov prediction in the LDA, $\mathcal{C}_{\rm LDA}$ (see text), and the solid line is $6.5 \times \mathcal{C}_{\rm LDA}$.

the expansion of an interacting Bose gas. We thus cannot exclude the possibility that the tails result from a modification of the beyond mean-field momentum distribution during the time-of-flight dynamics.

In order to further investigate the origin of the k^{-4} tails, we have studied their dependence upon the condensate density. The fitting parameter $\mathcal{C}_\infty$ of Eq. (4) is equal to the Tan contact constant [22,23], which, for a harmonically trapped gas, is found equal to $\mathcal{C}_{\mathrm{LDA}} = (64\pi^2/7)a_s^2 N_0 n_0$ in the LDA approximation [18]. The experimental results are plotted in Fig. 4 where the error bars reflect the uncertainty on $\mathcal{C}_\infty$ from the fit, as well as those on the calibration of N_0 and n_0 [18]. The fitted contact constant $\mathcal{C}_\infty/N_0$ per condensed particle is found proportional to n_0, as expected. The measured values of $\mathcal{C}_\infty$, however, are about 6.5 times larger than the expected value $\mathcal{C}_{\mathrm{LDA}}$. Note that in order to increase the density n_0 we increase the trapping frequency, which results in a decrease of the density of the central, dominant part of the distribution $n_\infty(k)$ measured after TOF. The observed proportionality between $\mathcal{C}_\infty/N_0$ and n_0 in spite of the variation of $n_\infty(k \simeq 0)$ rules out several possible spurious effects in the response of the MCP.

In conclusion, the measurement of the momentum distribution of a weakly interacting Bose gas released from a trap has allowed us to observe two components in the high momentum tails beyond the mean-field distribution. The first one is due to thermal depletion, and although some questions remain open, there are several observations which suggest associating the second one with the quantum depletion. The single-atom detection method of metastable helium gases is also able to provide signals of atom-atom correlations in momentum, a feature we intend to use in future investigations of momentum-space signatures of many-body effects.

We thank E. Cornell, Z. Hadzibabic, K. Mölmer, L. P. Pitaevskii, and S. Stringari for thorough discussions about the interpretation of our results. We thank F. Nogrette for providing support on the detector and M. Mancini for reading the manuscript. We acknowledge financial support from the Région Ile-de-France (DIM Daisy), the RTRA Triangle de la Physique, the European Research Council (Senior Grant Quantatop), the LabEx PALM (ANR-10-LABX-0039), the International Balzan Prize Foundation (2013 Prize for Quantum Information Processing and Communication awarded to A. Aspect), the Direction Générale de l'Armement, the french National Research Agency (ANR 15-CE30-0017-04) and the Institut Francilien de Recherche sur les Atomes Froids.

*To whom correspondence should be addressed.
david.clement@institutoptique.fr

[1] L. P. Sokol, in *Bose-Einstein Condensation*, edited by A. Griffin, D. W. Snoke, and S. Stringari (Cambridge University Press, Cambridge, England, 1995), p. 51.
[2] S. Utsunomiya, L. Tian, G. Roumpos, C. W. Lai, N. Kumada, T. Fujisawa, M. Kuwata-Gonokami, A. Loffler, S. Hofling, A. Forchel, and Y. Yamamoto, Nat. Phys. **4**, 700 (2008).
[3] F. Dalfovo, S. Giorgini, L. P. Pitaevskii, and S. Stringari, Rev. Mod. Phys. **71**, 463 (1999).
[4] S. W. Hawking, Commun. Math. Phys. **43**, 199 (1975).
[5] H. P. Yuen, Phys. Rev. A **13**, 2226 (1976).
[6] N. N. Bogoliubov, J. Phys. (USSR) **11**, 23 (1947).
[7] T. D. Lee, K. Huang, and C. N. Yang, Phys. Rev. **106**, 1135 (1957).
[8] R. J. Donelli, J. A. Donelli, and R. N. Hills, J. Low Temp. Phys. **44**, 471 (1981).
[9] R. Ozeri, N. Katz, J. Steinhauer, and N. Davidson, Rev. Mod. Phys. **77**, 187 (2005).
[10] M. Kohl, T. Stoferle, H. Moritz, C. Schori, and T. Esslinger, Appl. Phys. B **79**, 1009 (2004).
[11] K. Xu, Y. Liu, D. E. Miller, J. K. Chin, W. Setiawan, and W. Ketterle, Phys. Rev. Lett. **96**, 180405 (2006).
[12] J. T. Stewart, J. P. Gaebler, T. E. Drake, and D. S. Jin, Phys. Rev. Lett. **104**, 235301 (2010).
[13] C. Qu, L. P. Pitaevskii, and S. Stringari, arXiv:1608.08566.
[14] R. Chang, A. L. Hoendervanger, Q. Bouton, Y. Fang, T. Klafka, K. Audo, A. Aspect, C. I. Westbrook, and D. Clément, Phys. Rev. A **90**, 063407 (2014).
[15] Q. Bouton, R. Chang, A. L. Hoendervanger, F. Nogrette, A. Aspect, C. I. Westbrook, and D. Clément, Phys. Rev. A **91**, 061402(R) (2015).
[16] F. Nogrette, D. Heurteau, R. Chang, Q. Bouton, C. I. Westbrook, R. Sellem, and D. Clément, Rev. Sci. Instrum. **86**, 113105 (2015).
[17] M. Schellekens, R. Hoppeler, A. Perrin, J. Viana Gomes, D. Boiron, A. Aspect, and C. I. Westbrook, Science **310**, 648 (2005).
[18] See Supplemental Material at http://link.aps.org/supplemental/10.1103/PhysRevLett.117.235303 for details on the single-atom detection method, the Gross-Pitaevski numerics, the LDA calculation of the contact constant and the heating sequence.
[19] Y. Castin and R. Dum, Phys. Rev. Lett. **77**, 5315 (1996).
[20] Y. Kagan, E. L. Surkov, and G. V. Shlyapnikov, Phys. Rev. A **54**, R1753 (1996).
[21] L. Pitaevskii and S. Stringari, J. Low Temp. Phys. **85**, 377 (1991).
[22] S. Tan, Ann. Phys. (N.Y.) **323**, 2971 (2008).
[23] R. Combescot, F. Alzetto, and X. Leyronas, Phys. Rev. A **79**, 053640 (2009).
[24] We note that T_a may slightly differ from the gas temperature T in the regime $k_B T \simeq \mu$ due to the role of the Hartree-Fock potential induced by the condensate [3].
[25] Contact interactions between thermal atoms lead to a thermal contribution to the k^{-4} tails. The in-trap density of the thermal component is 2 orders of magnitude smaller than that of the condensate. The thermal contribution to the k^{-4} tails should thus be negligible.
[26] P. Makotyn, C. E. Klauss, D. L. Goldberger, E. A. Cornell, and D. S. Jin, Nat. Phys. **10**, 116 (2014).
[27] P. J. Leo, V. Venturi, I. B. Whittingham, and J. F. Babb, Phys. Rev. A **64**, 042710 (2001).